ORIGINAL PAPER

Shear wave velocity profiling by inverse analysis of array microtremors for two cities in Iran: conventional derivative-based versus genetic algorithm inversion methods

S. Mohammad Sadegh Sahraeian[1] · Ali Kavand[2] · Abbas Ghalandarzadeh[2]

Abstract

GA-based and conventional derivative-based inversion methods were employed to determine V_s profile of subsurface soil layers from array microtremors for two cities in Iran. The applied methods were verified against geotechnical and geophysical data. The results obtained by both GA-based and conventional inversions were in acceptable agreement with results of other V_s profiling techniques. However, the variability of obtained V_s data was smaller at deeper depths indicating more reliability of predictions. Comparison between seismic ground response based on V_s profiles of different methods showed that both GA-based and conventional inversion methods agree more with the seismic downhole method than the seismic refraction technique.

Keywords Shear wave velocity · Microtremor array measurement · Genetic algorithm · Inversion · f–k method · Dispersion curve · Rayleigh surface waves

1 Introduction

Shear wave velocity (V_s) is an important parameter which significantly affects dynamic response of sediments. The majority of current field test methods employed for determining V_s profile need drilling boreholes that may not be practical in all sites especially when deeper depths are of interest. Surface wave methods, on the other hand, are among those field test methods that enable the engineers to determine shear wave velocity structures without drilling any borehole. One of these surface wave procedures is the spectral analysis of surface waves (SASW) which was firstly introduced in the early 1980s (Heisey et al. 1982) and currently is being utilized in different places around the world (Fernández et al. 2011; Goh et al. 2011). Also, microtremor measurements as a passive type of surface wave methods have been recommended to assess not only the natural period and amplification

✉ Abbas Ghalandarzadeh
aghaland@ut.ac.ir

1 Civil and Environmental Engineering Department, Shiraz University of Technology, Shiraz, Iran

2 School of Civil Engineering, College of Engineering, University of Tehran, Tehran, Iran

ratio of sediments (Bard 1999; Nakamura 1989; Shafiee et al. 2011; Singh et al. 2017), but also the shear wave velocity profile of them (Apostolidis et al. 2004; Liu et al. 2000; Wu and Huang 2012; Pamuk et al. 2018; Rahman et al. 2018). Other types of surface waves methods such as MASW or MSOR have also been applied for estimation of V_s profile of subsurface layers (Tokeshi et al. 2013). Furthermore, a few researchers combined different surface waves approaches and developed more sophisticated methods to estimate V_s profiles. For example, recently, Lontsi et al. (2016) combined surface wave phase velocity dispersion curves and horizontal-to-vertical (H/V) spectral ratio of microtremors for subsurface site characterization.

Surface wave procedures are based on the dispersion characteristics of Rayleigh surface waves in layered media. The relation between the velocity and frequency or wavelength of the propagating wave is referred to as dispersion. In other words, while the penetration depth of surface Rayleigh waves increases due to an increase in wavelength, the dispersion takes place. Generally, because the Rayleigh waves with short wavelength (high frequencies) propagate only in a superficial zone near the ground surface, their propagation velocity is mostly affected by the properties of the shallower soil layers. But while the waves with long wavelength penetrate deeply into the ground, their propagation velocity depends on the specifications of deeper layers. In other words, the velocity of propagation of Rayleigh waves reflects the properties of those layers where the major part of the wave propagates.

In order to specify a dispersion curve of surface waves by microtremor measurements, ambient vibrations of the ground are recorded in a wide range of frequencies. V_s profile of the ground is then obtained from the experimental dispersion curve by a mathematical algorithm known as inversion. During the inversion process, the properties of subsoil layers (commonly, thickness and shear wave velocity) are adjusted in an iterative procedure to match the theoretical dispersion curve with the experimental one. For this purpose, firstly, a fitness function which represents the deviation between the experimental and theoretical dispersion curves is defined. Subsequently, the best fit between the experimental and theoretical dispersion curves is detected based on an optimization scheme which minimizes the fitness function. Finally, the best-fit parameters in the theoretical model are chosen as the ultimate V_s profile of the site.

Up to now, many studies have been conducted on the inversion of experimental dispersion curve of Rayleigh waves. For example, Horike (1985) presented an inversion procedure of phase velocity of microtremors for estimation of V_s profiles in urban areas. Tokimatsu et al. (1992) utilized an inversion process which incorporated the effects of multiple Rayleigh modes on the recorded dispersion data and used it for estimation of V_s profile. Lai and Rix (1998) reported a comprehensive study on simultaneous inversion of Rayleigh phase velocity and attenuation for near-surface site characterization. Arai and Tokimatsu (2004) applied an inversion analysis of the horizontal-to-vertical (H/V) spectrum of microtremors to estimate V_s profiles for representative sites. Kavand et al. (2006) investigated the reliability of the V_s profiles obtained by inversion of array microtremors in Bam city, southeast of Iran, and concluded that the inverted V_s profiles compare well with the results of other methods. Kocaoglu and Firtana (2011) presented an inversion of spatial autocorrelation coefficients (SPAC) of array microtremors to estimate V_s profile of subsoil layers.

Moreover, a number of the previous researches have focused on advanced nonlinear inversion procedures such as genetic algorithm, simulated annealing (Kolar 2000) and neighborhood algorithm (Sambridge 1999), rather than the conventional linear inversion methods. It should be noted that the objective function in the inversion of surface wave data shows multiple local minimum and maximum which can potentially lead to failure

of the inversion, especially when the starting model is adjacent to a local minimum which has a potential to attract the solution. As a result, a critical issue in the inversion of surface wave data is its dependency on an initial model. In cases that an initial information of subsurface soil profile is available, a proper primary model can be estimated and the linear conventional inversions can recognize the global minimum of the fitness function as an optimal solution, while if this reliable information is not available, the conventional inversion procedures may choose a local optimal solution. Genetic algorithm (GA) as a nonlinear optimization method can effectively overcome these problems since it is capable to simultaneously seek local and global optimum solutions. GA, which has many applications for optimization problems in various fields of engineering, has recently been applied in the inversion of surface waves data (Goldberg 1989). Yamanaka and Ishida (1996) examined the applicability of GA-based inversion of short and intermediate period surface wave dispersion data for estimation of V_s profile of sediments. Also, a new GA-based inversion for spectral analysis of surface waves (SASW) has been employed by Hunaidi (1998) and Pezeshk and Zarrabi (2005). Pezeshk and Zarrabi (2005) used GA to invert experimental dispersion curves obtained by SASW method. They investigated the reliability of this approach and reported a good agreement between the estimated V_s profiles and the results of other methods including seismic downhole survey. Dal Moro et al. (2007) utilized an inversion of Rayleigh wave dispersion curve via GA. In their study, shear wave velocity profiles resulted from the inversion process were approved by borehole stratigraphy. Also, successful applications of GA-based inversion of array microtremors were reported by Kuo et al. (2016) and Sahraeian et al. (2008, 2012) for deriving shear wave velocity structure of the ground in rural areas. Moreover, Picozzi and Albarello (2007) utilized a joint inversion of surface waves data to assess V_s structure of subsoils. They combined the nonlinear genetic and linearized algorithms to overcome the problems of each approach while improving the estimation of subsurface structure.

In current study, a recently developed nonlinear inversion method that uses genetic algorithm (GA) is adopted and examined to reduce the inherent difficulties in the inversion procedure of microtremor dispersion data. Another objective of this study is to use GA-based method as a derivative-free technique and to compare the results with the conventional derivative-based approach. For this purpose, a series of array microtremor measurements were conducted in two different cities in Iran, namely, Urmia in northwest and Bam in southeast. It should be noted that Bam city was extensively destroyed by a destructive earthquake in December 2003. Using the array measurements, V_s profiles of sedimentary deposits in both cities are determined by inverse analysis of dispersion curves of microtremors via both conventional and GA-based approaches. Finally, the reliability of these two inversion procedures is assessed, comparing inverted V_s profiles with other available data, while the advantages of each method are discussed.

2 Estimation of V_s profile of subsoil using array measurement of microtremors

The estimation of V_s structure of sediments by array measurement of microtremors includes three main steps: (1) recording microtremors, (2) determination of experimental dispersion curve and (3) using inversion analysis of the experimental dispersion curve to obtain V_s profile of subsoil.

2.1 Array measurement of microtremors

Array measurement of microtremors as a passive surface waves technique does not need generation of artificial vibrations. Instead, three-component motions of ambient vibrations are recorded using an array of sensors placed on the ground surface. A sample setup for array measurement of microtremors is shown in Fig. 1. As this figure indicates, the setup includes a number of three dimensional velocity sensors along with a data logger and a portable computer. The data logger digitizes the recorded microtremor data and stores it on the computer in the field. The sensors can be placed on the ground surface in parallel circular patterns with almost the same spacing between them around a circle, while one of them is usually placed at the array center. It should be noted that the array may not necessarily have a circular configuration; however, it is better to maintain it as much circular as possible (Tokimatsu 1995). Also, irregular geometries might be utilized (Marano et al. 2014) to overcome practical limitations in the field such as the presence of obstacles.

Since the range of wavelengths in which reasonable phase velocities can be obtained is a function of the distance between the sensors, some researchers suggest that the array configuration should satisfy Eq. 1 to achieve reliable results.

$$D_{\max} > \lambda_{\max}/3, \quad D_{\min} < \lambda_{\min}/2 \tag{1}$$

In this equation, $D_{\max}$ and $D_{\min}$ are, respectively, the maximum and minimum spaces between the sensors, while $\lambda_{\max}$ and $\lambda_{\min}$ are in turn the maximum and minimum effective wavelengths. In order to obtain intended range of wavelengths or phase velocities, microtremor measurements should be repeated using different array sizes or initially be placed in a parallel circular pattern as shown in Fig. 1. More details regarding the procedure of array measurement of microtremors may be found elsewhere (e.g., Marano et al. 2014; Tokimatsu 1995).

2.2 Determination of experimental dispersion curve

In a layered elastic media, the relation between the wave velocity, usually referred to as phase velocity (c), and the frequency (f) and wavelength (λ) is expressed by the following equation:

$$c = \frac{\lambda}{T} = f\lambda \tag{2}$$

The variation of phase velocity with wavelength or frequency is called dispersion, and the diagram which specifies this variation is referred to as the dispersion curve. In order
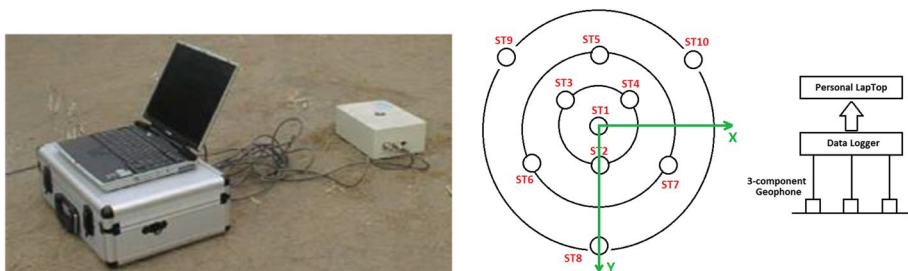

Fig. 1 Typical instrumentation setup for array measurement of microtremors

to determine the dispersion curve of the vertical component of microtremors, high-resolution frequency-wavenumber (*f–k*) spectrum analysis firstly introduced by Capon (1969) is adopted in current study. The *f–k* spectrum, $P(f, k)$, is specified by Eq. 3:

$$P(f,k) = \sum_{i=1}^{M} \sum_{j=1}^{M} A_i^*(f,k)A_j(f,k)G_{ji}(f) \exp[ik(x_i - x_j)]$$ (3)

In the above equation, M is the total number of sensors; x_i is the vector position of ith sensor; * denotes complex conjugate; f is the frequency; k is the vector wavenumber defined as $k = |k|\exp(i\theta)$; and θ is the azimuth of the vector wavenumber. $G_{ij}(f)$ is the cross-power spectrum between ith and jth sensors at a frequency of f, which is defined as $G_{ij}(f) = 1/N \sum_{n=1}^{N} S_{in}(f)S_{jn}^*(f)$, where N is the total number of the nonoverlapping data segments, and S_{in} is the Fourier transform of the data in the ith sensor and in the nth segment. A_i is calculated according to following relationship:

$$A_i(f,k) = \sum_{j=1}^{M} q_{ij}(f,k) / \sum_{i=1}^{M} \sum_{j=1}^{M} q_{ij}(f,k)$$ (4)

In this equation, $q_{ij}(f, k)$ is the inverse of the matrix $exp[ik(x_i - x_j)]G_{ij}(f)$.

The *f–k* spectrum can be plotted in a 2D wavenumber ($K_x - K_y$) diagram for each frequency. The peak of the spectrum that occurs at frequency f and distance $\left|k_p\right|$ from the origin, can be used to calculate the corresponding phase velocity (c) and wavelength (λ) implementing below formulations:

$$c = 2\pi f / \left|k_p\right|, \quad \lambda = 2\pi / \left|k_p\right|$$ (5)

The above calculations should be repeated for different frequencies to obtain the dispersion curve for the whole frequency range of interest. Further details regarding this procedure can be found elsewhere (e.g., Capon 1969; Tokimatsu 1995). In this study, we prepared a computer program in MATLAB based on the preceding formulations to determine the dispersion curves. A representative *f–k* spectrum calculated based on the aforementioned procedure is shown in Fig. 2 as contours of $P(f,k)/P_{\max}(f,k)$ where $P_{\max}(f,k)$ denotes maximum value of the *f–k* spectrum. The spectrum is presented for a representative frequency of 10 Hz which attains its peak at $K_x = -0.40$ rad/m and $K_y = 0.21$ rad/m corresponding to a phase velocity of 139 m/s. It should be noted that in current study, the vertical component of recorded microtremors is used; thus, the obtained dispersion curves correspond to Rayleigh waves.

2.3 Inversion procedure

The most important and challenging part of estimation of shear wave velocity profile by microtremor array method is the inversion procedure. This procedure includes two main steps. The first step is to utilize a theoretical solution, commonly the one formulated by Haskell (1953), to determine the theoretical dispersion curve, while in the second step, the theoretical dispersion curve is adjusted to match the experimental dispersion curve. The fitted theoretical dispersion curve provides the optimum shear wave velocity profile which depends on a set of adjustable parameters, e.g., shear wave velocities and thicknesses of the soil layers. The Haskell's formulation deploys a number of intrinsic parameters of soil layers based on which a relation between the phase velocity (c) and
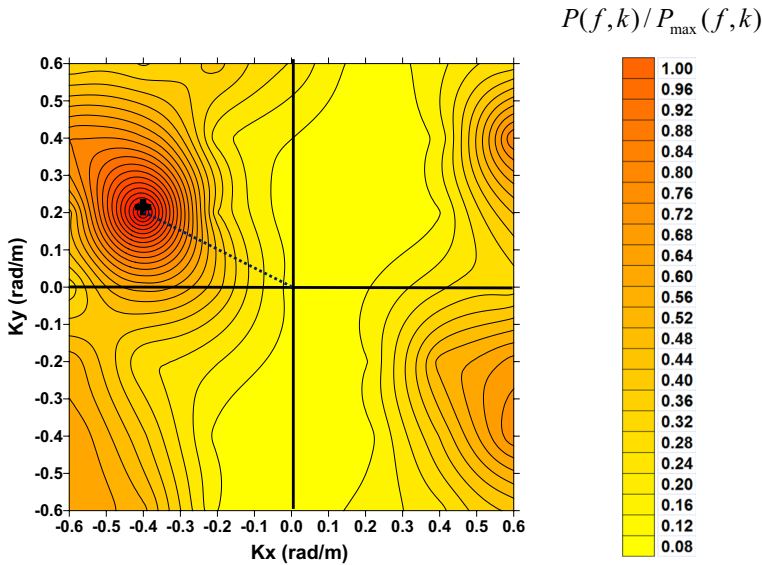
Fig. 2 Representative *f*–*k* spectrum at frequency of 10 Hz showing a peak at $K_x = -0.40$ rad/m and $K_y = 0.21$ rad/m

the wavenumber (*k*) or alternatively a dispersion curve can be derived. The general form of the equation for development of a dispersion curve can be written as below (Pezeshk and Zarrabi 2005):

$$F[\lambda_m, \mu_m, \rho_m, k, d_m, c] = 0 \tag{6}$$

where λ_m and μ_m are Lame's elastic constants of each soil layer, ρ_m is the mass density of soil layers, *k* is the wavenumber which is equal to $2\pi/\lambda$, d_m is the thickness of soil layers, *c* is the phase velocity, and *m* denotes the total number of soil layers. It is worth noting that λ_m and μ_m can be accordingly replaced by P-wave velocity (V_P) and S-wave velocity (V_s). While V_P, V_s, d_m and ρ_m are known for all layers, Eq. 6 can be solved to obtain the theoretical dispersion curve. However, practically, the values of V_P and ρ_m have minor effects on the theoretical dispersion curve (Rix et al. 1991; Tokimatsu et al. 1992); thus, their variations can be ignored in the inversion process. As a result, Eq. 6 can be simplified as:

$$F[V_s, d, c, f] = 0 \tag{7}$$

In this equation, V_s and *d* are a set of shear wave velocities and thicknesses of the considered soil layers. In this paper, a computer program was developed in MATLAB to solve Eq. 7 and determine the theoretical dispersion curve.

2.3.1 Conventional inversion

The objective of conventional inversion procedure is to detect a soil profile which minimizes the least-squares equation defined as follows:

$$\sum_{i=1}^{I} \left(c_i^{\text{experimental}} - c_i^{\text{theoretical}} \right)^2 = \text{minimum} \tag{8}$$

where $c_i^{\text{experimental}}$ is the observed phase velocity at frequency i for all I different frequencies obtained from Eq. 5, while $c_i^{\text{theoretical}}$ is the theoretical phase velocity at frequency i, for the fundamental mode of Rayleigh waves calculated from Eq. 7.

Formerly, different methods have been proposed for solving Eq. 8 such as the nonlinear optimization method proposed by Dorman and Ewing (1962). In current research, we formulated this nonlinear inversion method in a MATLAB code, in which the layered medium is deemed to be horizontally stratified consisting of N layers with different properties. As mentioned earlier, because of the negligible influences of mass density and P-wave velocity on the dispersion characteristics, these parameters were assumed to be fixed and only the shear wave velocities and thicknesses were sought during the inversion process. Therefore, the total number of unknown values, J, was $2N-1$ assuming that the bottom layer is the half-space whose V_s value is unknown. In this case, the governing equation of the inversion problem in matrix form can be expressed as (Tokimatsu 1995):

$$P_{I \times J} \Delta A_{J \times 1} = C_{I \times 1} \tag{9}$$

where $\Delta A_{J \times 1}$ is the correction vector for $A_{J \times 1}$ which is a column vector whose elements are the initial values of the unknown parameters (a_j). $P_{I \times J}$ is a matrix with elements equal to $\partial c_i^{\text{theoretical}} / \partial a_j$, and $C_{I \times 1}$ is a column vector whose elements are $C_i^{\text{experimental}} - C_i^{\text{theoretical}}$. During the inversion process, the correction vector (ΔA) is obtained from Eq. 9; then, matrix A is updated with $A + \Delta A$, and this procedure is repeated until the assumed soil model satisfies the least-squares equation defined in Eq. 8. To know further details regarding this procedure, one can refer to Tokimatsu (1995).

2.3.2 Genetic algorithm-based inversion

2.3.2.1 Fundamentals of genetic algorithm Holland (1975) was among the first researchers who introduced genetic algorithms (GAs) during the 1970s. The basic concept behind this optimization approach is Darwinist theory, a genetically based evolutional plan that the fittest survive and propagate, while the others vanish. The GA-based inversion can be more reliable because it does not require an initial model to start the optimization. Also, it works on objective function for optimization and does not depend on gradient information. This method optimizes the desired function by considering a group of possible solution instead of a single solution.

In GA optimization approach, firstly, a population (generation) of variables are randomly produced. Then, the variables are divided into different sets. Each set of variables named string (chromosome) includes some characters (gen). Every character is a variable of the objective function, and each string is a possible solution for the problem. The characters are binary numbers, but they are changed to real numbers before evaluation by the objective function. A mathematical value called fitness function that is calculated by applying a string (solution) into the objective function represents the efficiency of each string for the problem (objective function). A solution which is more suitable for the problem earns more value of fitness function, and those with less compatibility with the problem get less values. Finally, similar to the nature, the best strings (solutions) survive and produce the next population of the solutions, while the inappropriate ones disappear.

After production of initial population of solutions randomly, the next generations are produced considering the first generation. For this purpose, four genetic operators are used: (1) Selection, (2) Crossover, (3) Mutation and (4) Elitism. In each generation, the solutions are selected based on their fitness and mate in order to generate the next generation. In other words, fitter parameters mate more than the others. In such a way, the proper solutions remain and reproduce, while the inappropriate ones gradually disappear. The selection operator refers to the method of choosing the parameters in each generation. In crossover operator, two selected chromosomes (parents) are divided into sections and some sections of the first parent are substituted by the corresponding sections of the second one. Mutation operator causes an incidental change of chromosomes (parameters) in order to generate new parameters randomly. The main purpose of this operator is to reduce the possibility of focusing on a small group of parameters during the searching process (Man et al. 2012). The last operator, called elitism, certifies the survival of fittest parameters (chromosomes) by transferring them without any change to the next generation. This operator causes existence of best chromosomes in next generations and their participation in breeding of new parameters. Finally, the GA procedure can be terminated after a predetermined number of generations or when a preset value for the fitness function will be obtained. Obviously, the final parameter that satisfies this criterion is the optimum solution for the objective function. In this study, we utilized a code which was developed via the Genetic Algorithm TOOLBOX of MATLAB for GA-based inversion of experimental dispersion curves.

2.3.2.2 Inversion procedure by genetic algorithm During a GA-based inversion, deviation of the theoretical dispersion curve from the experimental one is measured by the following equation which is also known as error function:

$$\text{Error} = \sum_{i=1}^{I} \left(c_{\text{experimental}} - c_{\text{theoretical}} \right)^2 \tag{10}$$

where $c_{\text{experimental}}$ and $c_{\text{theoretical}}$ are the column vectors of experimental and theoretical phase velocities, respectively. The dimensions of both these vectors are $I \times 1$, where I is the total number of frequencies considered in the inversion. The final goal of optimization procedure is to minimize the error function. The optimization problem is subjected to a search space for each unknown parameter (i.e., thickness and shear wave velocity of each layer), while the search space is kept limited by applying constraints on the variations of the unknown parameters.

3 Case studies

In order to examine the reliability and effectiveness of two previously mentioned inversion approaches, two case studies are presented and discussed herein. These examples include array observations of microtremors in Bam and Urmia cities in Iran which are considered to describe the applicability of the proposed inversion procedures for determination of reliable V_s profiles of sediments.

3.1 Bam city

3.1.1 Microtremor measurements

Microtremor measurements in Bam city, south east of Iran, were performed after the destructive Bam earthquake of 2003. The measurements included 5 array and 49 single-point observations distributed over the area; however, only the array measurements are discussed herein. Locations of microtremor observation points are depicted in Fig. 3. Microtremors were recorded by three-component seismometers with natural frequency of 0.5 Hz which were able to measure the ground velocity in two horizontal and vertical directions.
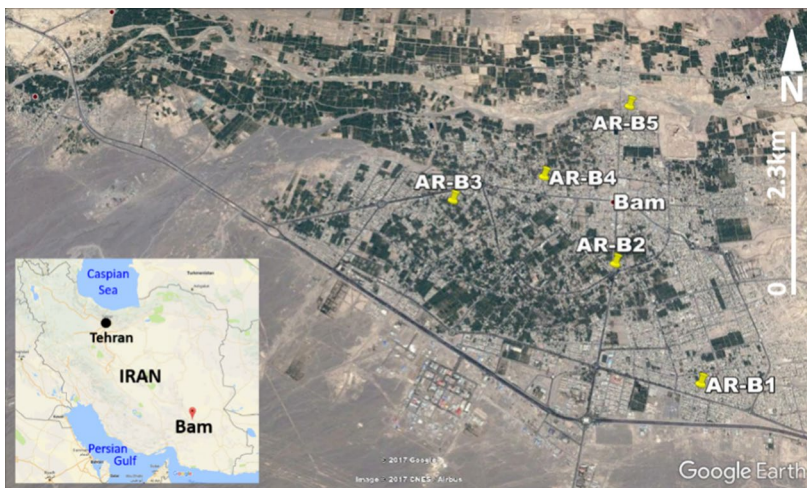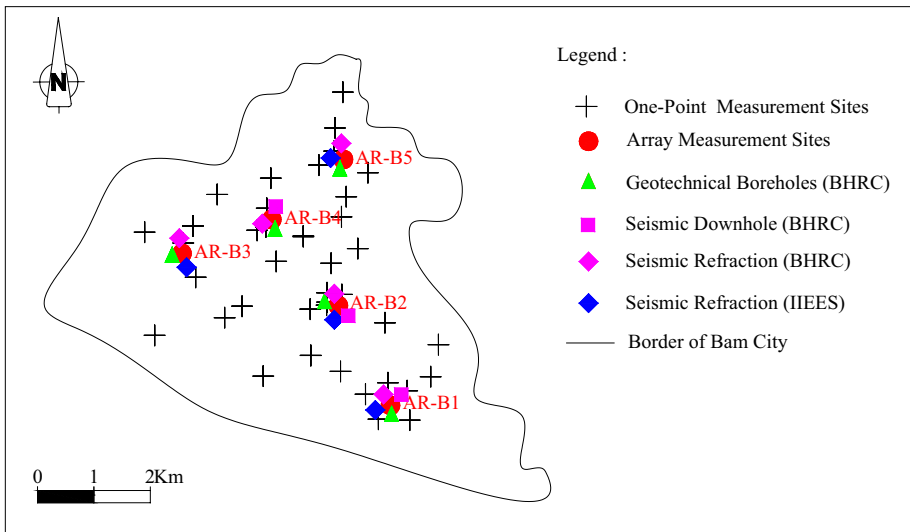
Fig. 3 Locations of microtremor observation points in Bam city

The response of seismometer was desirably flat over frequencies greater than 1.0 Hz. The configuration of employed arrays was kept as much circular as possible; however, in some array stations, irregular patterns were inevitably used to exclude the encountered obstacles. The spacing between the sensors varied from 10 m to 520 m at different locations where at least five sensors were employed in each array and a sensor was installed at the array center as the reference point. The smaller spacing was adopted so that the shallow depths of interest in geotechnical characterization can be included in inversion process. Ground vibrations were observed for 2.0 min at the midnight to keep the man-made noises as minimum as possible, and at each station, the measurements were repeated twice, to capture the variation of recorded signals. The sampling frequency was selected as 100 Hz, and the orientation of seismometers in all arrays was kept N–S. Moreover, all seismometers of the arrays were synchronized using GPS timing.

3.1.2 V_s profiling

In order to obtain the experimental dispersion curves, previously introduced *f–k* analysis was implemented using six data segments of 20 s duration in each single analysis. Note that, since the microtremor measurements were repeated twice in each array, two series of dispersion curves were obtained, while their average values were consequently used for inversion. Figure 4 shows final experimental dispersion curves for all arrays in Bam city.

Geotechnical and geophysical studies in Bam city generally show that variation of soil layer properties with depth in most parts of the city is not too much complicated (Ghalandarzadeh et al. 2004). As a result, for simplicity, the analytical soil models in all sites were assumed to consist of four distinct horizontally stratified layers overlying an elastic half-space. However, in site AR-B5, five layers were considered to capture the variation of V_s with depth in more details especially at shallow depths. Because both shear wave velocities and thicknesses were sought, the total number of unknown parameters was nine for site AR-B5 and seven for the others. In the inversion process, the constraints on soil properties were chosen in such a way that limit them to physically reasonable values, but being wide enough allowing them to be further tuned to determine the optimized solution. For the start model, layers of equal thicknesses in top 50 m was assumed and their initial V_s values were tuned according to the general trend of the dispersion curve at each point based on the associated wavelengths for each frequency as suggested in previous investigations (e.g., Richart et al. 1970). Figure 4 depicts the theoretical dispersion curves of the inverted soil profile at the end of conventional inversion process along with the experimental dispersion curves. As can be seen, a close match is observed between the two series of curves confirming that the inversion process has converged successfully. Figure 5 shows final mean and mean ± one standard deviation of shear wave velocity profiles as obtained from the inverse analyses along with the start models used in the inversion process. Referring to Fig. 5, it is observed that all inverted profiles reach to the engineering seismic bedrock where a layer with a V_s value of greater than 750 m/s is located.

For GA-based inversion, the target input data consist of the abscissas of experimental dispersion curve at 21 phase velocities. A population size of 50 was run for more than 200 generations. The probability of crossover was initially selected as 80%; however, by progression of the inversion procedure, it was further reduced. At each generation, four individuals were produced by elitism strategy, while the remainder of them was produced by mutation. Figure 6 shows experimental and the best-match theoretical
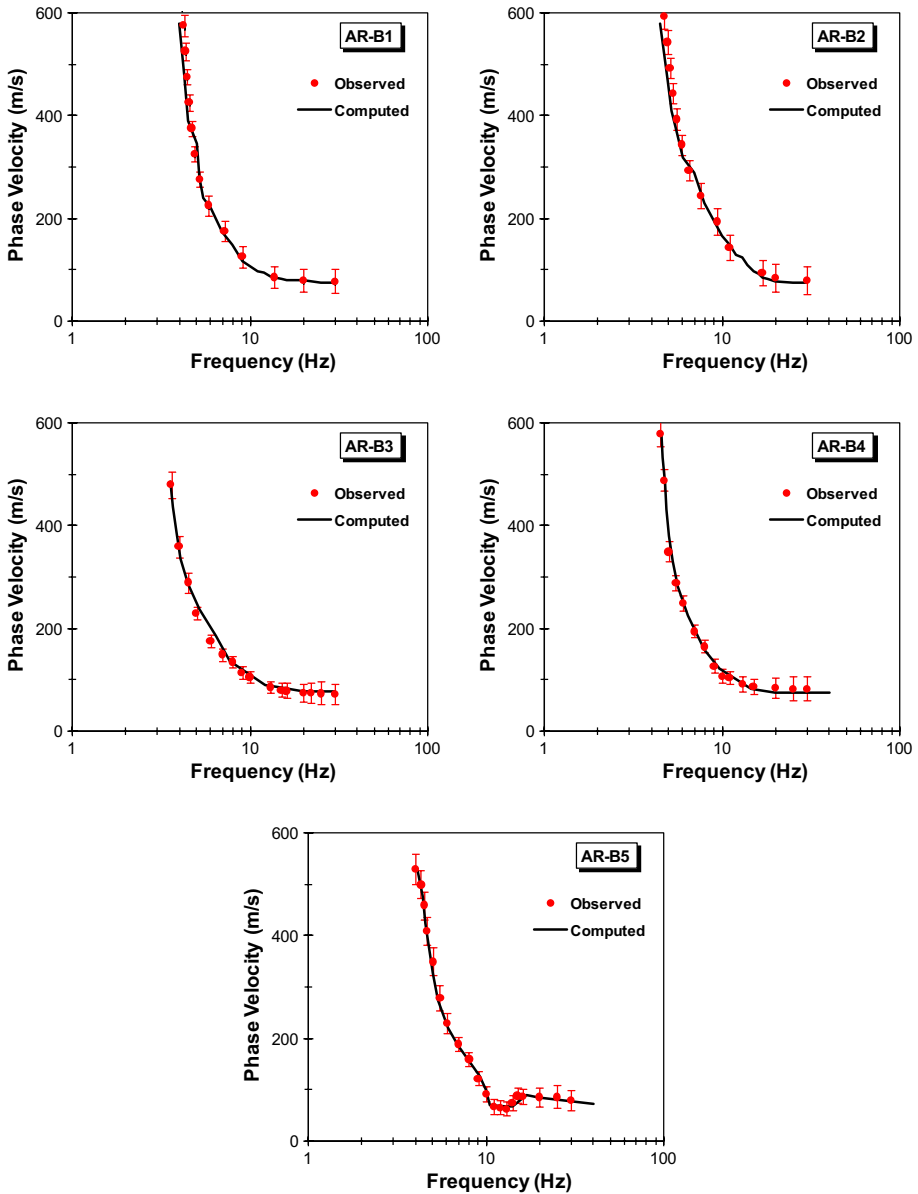
Fig. 4 Comparison between experimental and theoretical dispersion curves after convergence of conventional inversion for Bam city (error bars show mean values ± one standard deviation)

dispersion curves along with their corresponding convergence histories. It can be observed that the inversion analyses converged after about 30 generations. Figure 7 summarizes all inverted shear wave velocity profiles obtained by GA-based inversion
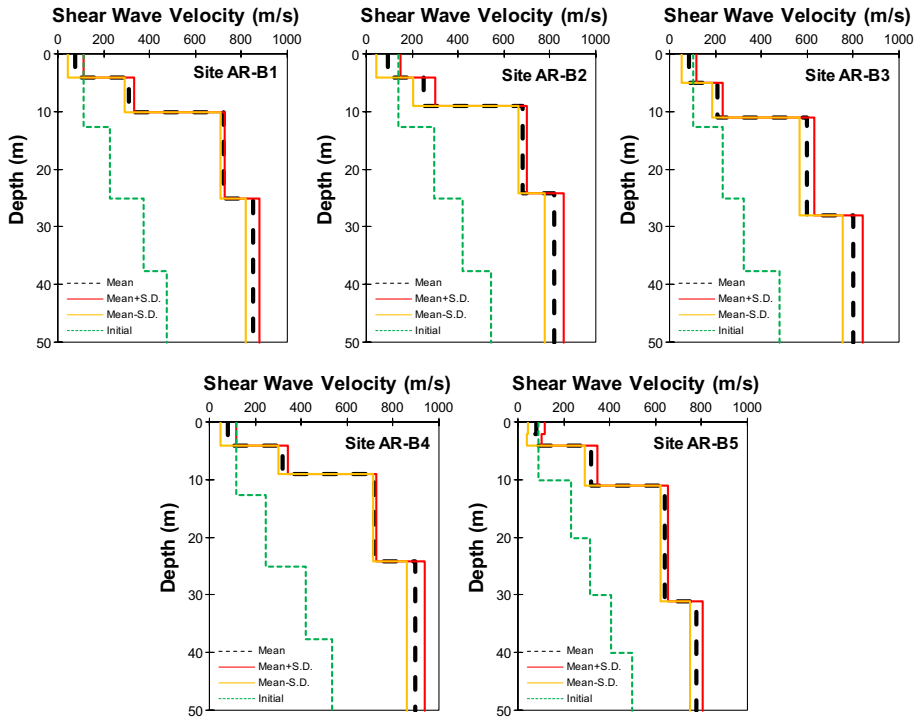
Fig. 5 Inverted V_s profiles in Bam city obtained by conventional inversion

approach in Bam city in terms of mean and mean ± one standard deviation of shear wave velocities.

3.2 Urmia city

3.2.1 Microtremor measurements

Array measurement of microtremors in Urmia city, northwest of Iran, was conducted at 5 sites during the seismic microzonation study of the city in 2002 (Ghalandarzadeh 2002). Figure 8 shows the location of microtremor measurement points throughout Urmia city. Microtremors were recorded by three-component seismometers with natural frequency of 0.5 Hz and desirably flat response over frequencies greater than 1.0 Hz.

The array configurations were circular for one array, while two triangular and two irregular patterns were also employed. The spacing between the sensors varied between 10 and 400 m at different locations where five sensors were employed within the arrays with a reference sensor always kept at the array center. Ground vibrations were observed at the midnight to keep the unwanted human noises minimal, and at least five recordings of two minutes duration were obtained at each station to capture the variation of recorded signals. The sampling frequency was 100 Hz, and the orientation of seismometers in all arrays was N–S. In addition, all seismometers of the arrays were synchronized using GPS timing.
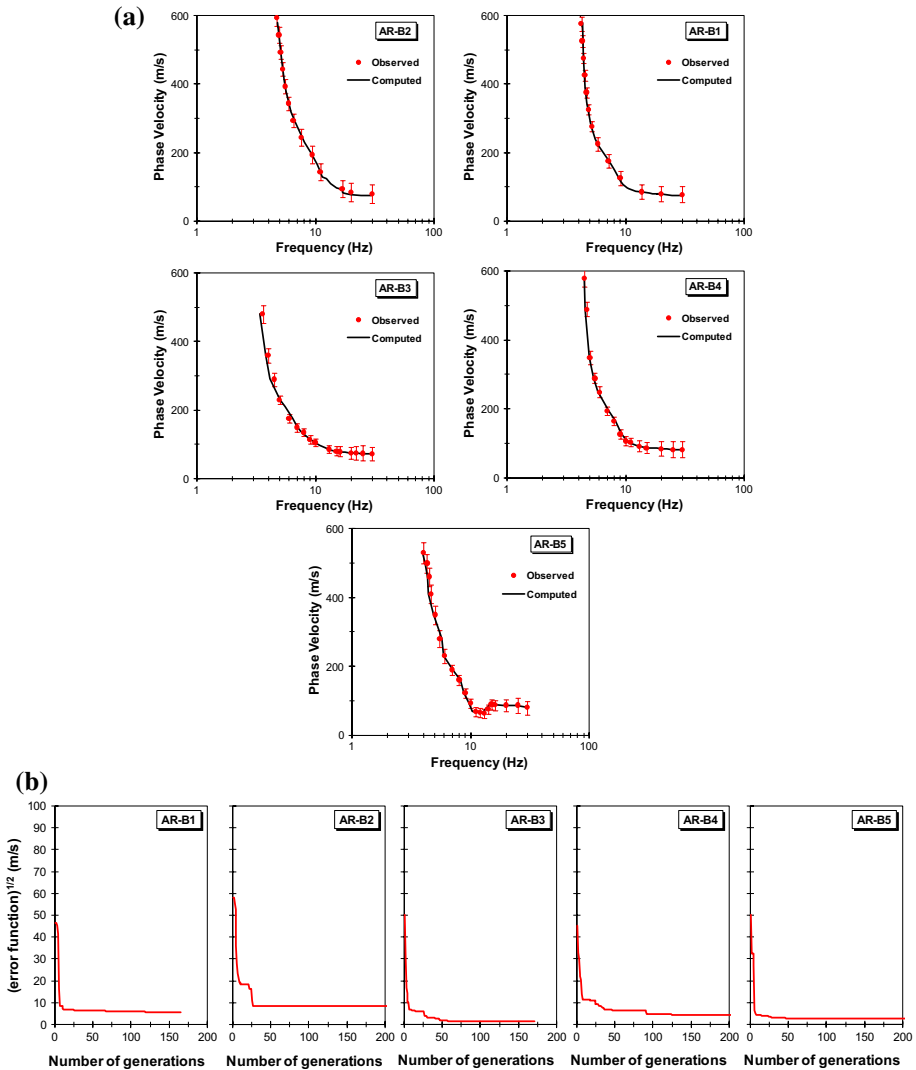
Fig. 6 **a** Experimental and the best-match theoretical dispersion curves for Bam city (error bars show mean values ± one standard deviation), **b** the corresponding convergence histories

3.2.2 V_s profiling

As mentioned previously, the *f–k* analysis was used to obtain the experimental dispersion curves. For this purpose, six data segments of 20 s duration were used in each series of analyses and the final dispersion curve for each array was obtained by averaging all dispersion curves obtained from repeated measurements in the array. Final experimental dispersion curves for all arrays in Urmia city are presented in Fig. 9.

The analytical soil models in all sites were assumed to consist of four distinct horizontally stratified layers overlying an elastic half-space. Therefore, the total number of initial unknown
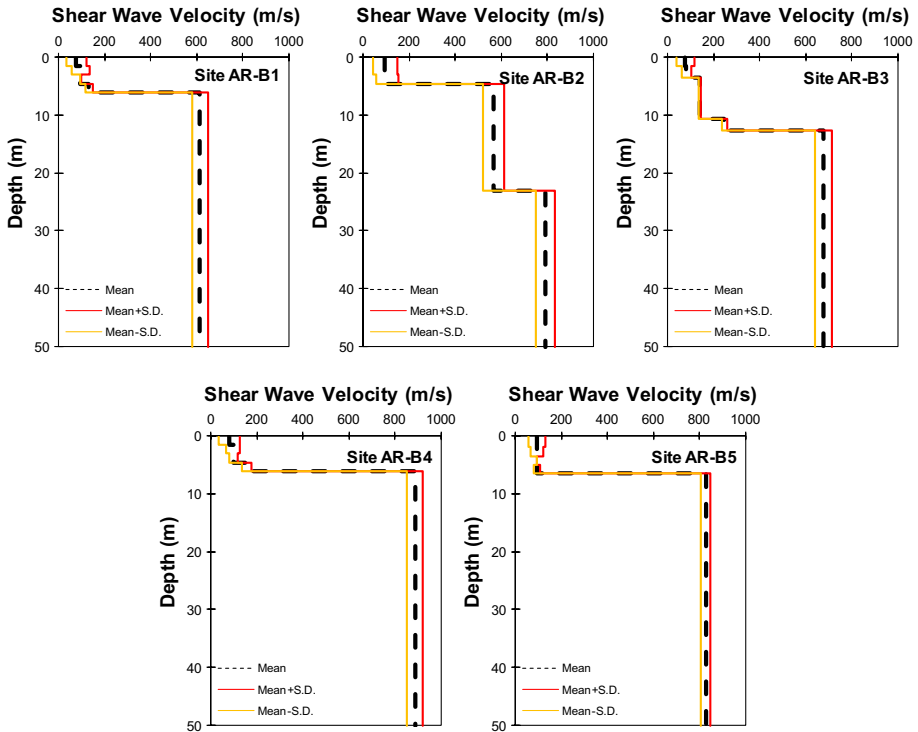
Fig. 7 Inverted V_s profiles in Bam city obtained by GA-based inversion

variables in both conventional and GA-based inversions was nine including four thickness values and five shear wave velocity values; however, in GA-based method, the final optimum model of soil layers in AR-U5 included four different layers. Since, the employed inversion procedure for Urmia city is entirely similar to what previously described for Bam city, only final inversion results are addressed in this section. Figure 9 presents the theoretical dispersion curves of the inverted soil profile at the final stage of conventional inversion along with their corresponding experimental dispersion curves. According to this figure, a close match is observed between the two series of curves showing successful convergence of the inversion process. All shear wave velocity profiles obtained by the conventional inverse analyses are shown in Fig. 10. The inverted data are specified for both mean and mean±one standard deviation. The start models used in the inversion process are also shown in Fig. 10. As one may notice, all inverted profiles reach to the engineering seismic bedrock. Figure 11 shows the experimental and the best-match theoretical dispersion curves along with their associated convergence histories obtained during GA-based inversion. Figure 12 shows all inverted shear wave velocity profiles obtained by GA-based inversion approach in Urmia city in terms of mean and mean±one standard deviation of shear wave velocities.
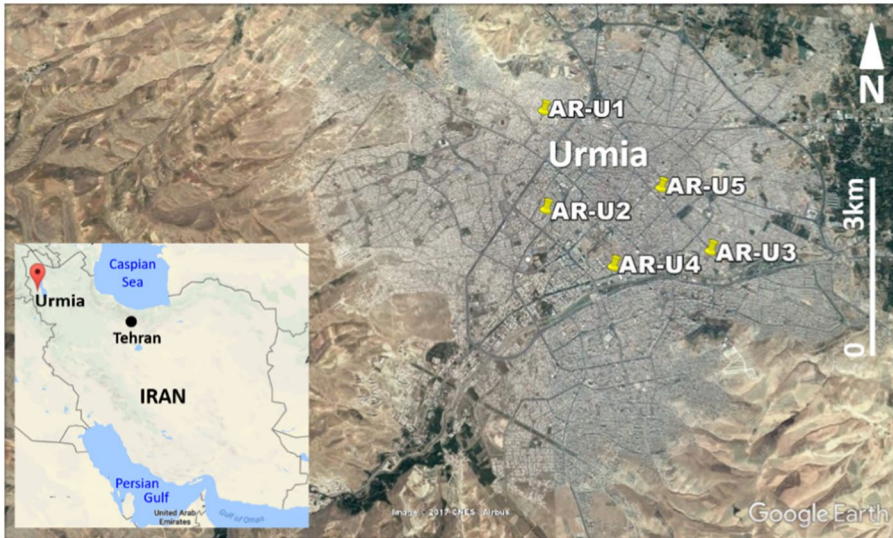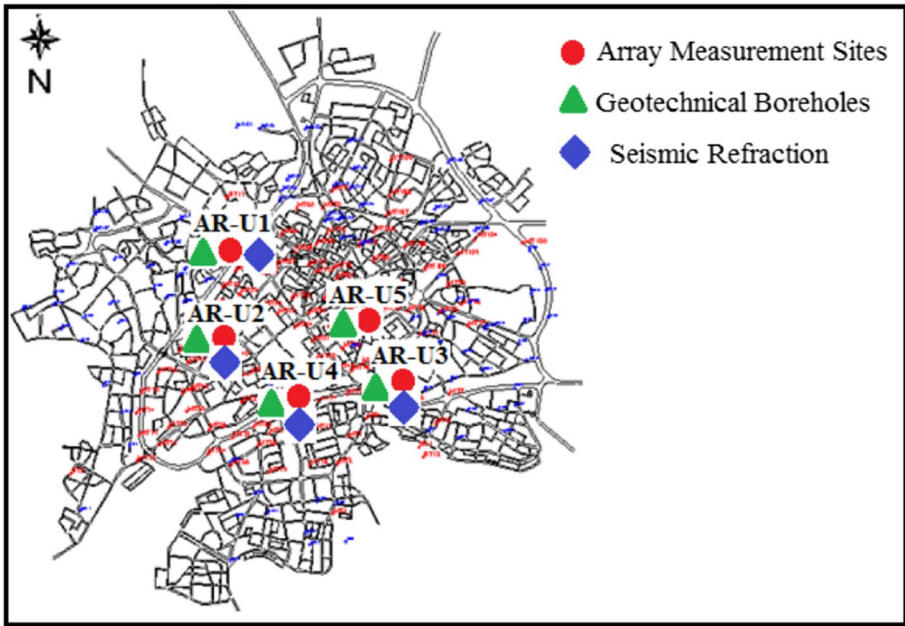
Fig. 8 Microtremor observation points in Urmia city

3.3 Reliability of inverted V_s profiles

In order to investigate the reliability of the conventional and GA-based inversion methods, comparisons were made between the inverted V_s profiles and those based on geophysical and geotechnical techniques. The details are discussed in following parts.
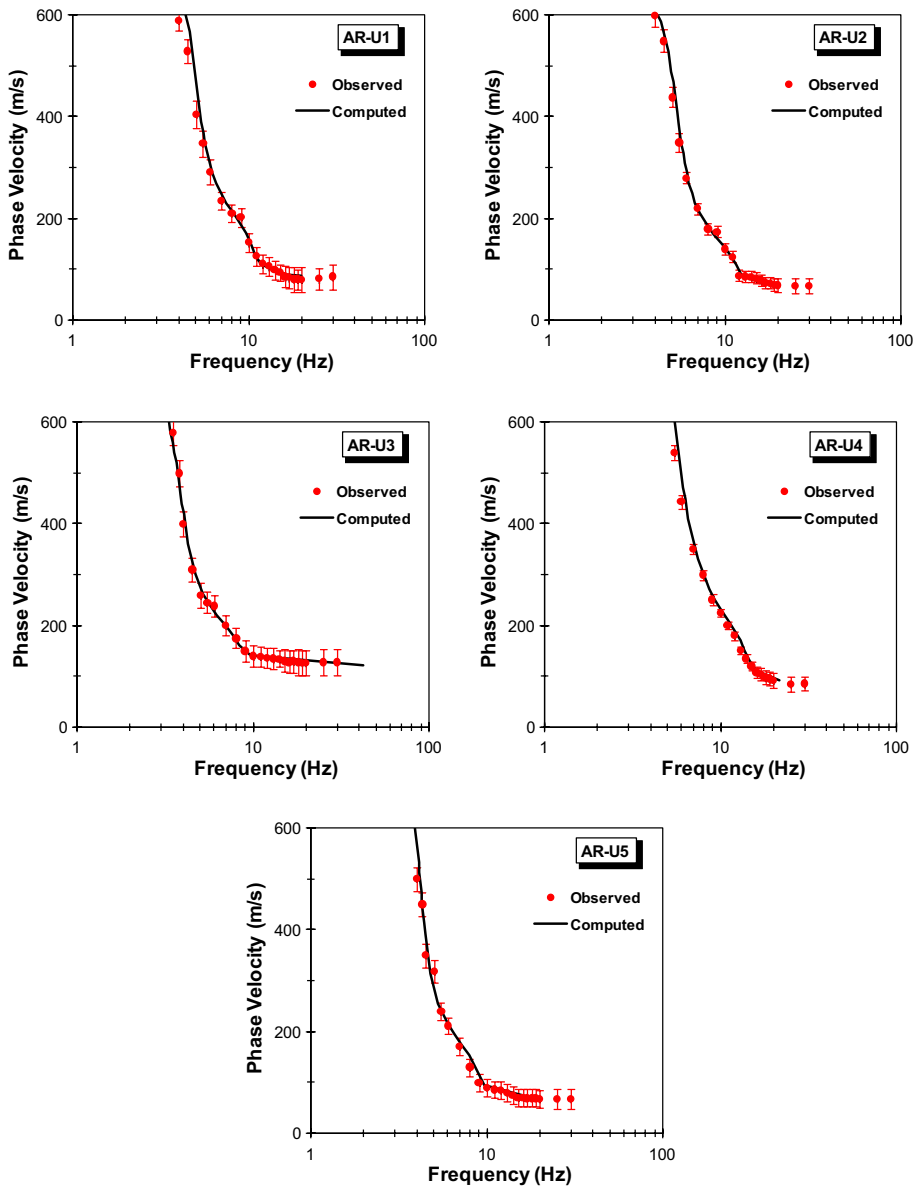
Fig. 9 Comparison between experimental and theoretical dispersion curves after convergence of conventional inversion for Urmia city (error bars show mean values ± one standard deviation)

3.3.1 Bam city

The Building and Housing Research Center (BHRC) of Iran had drilled several geotechnical boreholes along with extensive geophysical seismic refraction and downhole surveys throughout Bam city after the destructive earthquake of 2003 as part of a comprehensive seismic microzonation project (Tabatabaii et al. 2003). Moreover, International Institute of
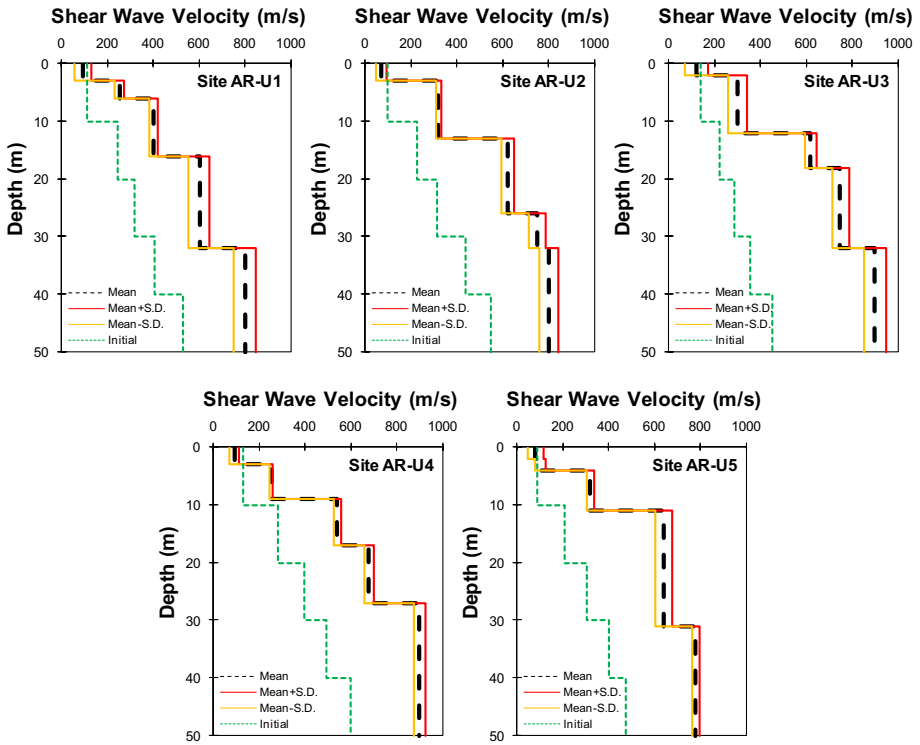
Fig. 10 Inverted V_s profiles in Urmia city obtained by conventional inversion

Earthquake Engineering and Seismology of Iran (IIEES) had carried out a series of seismic refraction surveys throughout Bam city. A number of BHRC and IIEES survey points are located nearby the array sites of current study. All these data can be utilized as a benchmark to evaluate the reliability of the inverted V_s profiles.

Schematic geotechnical stratigraphy at the boreholes drilled by BHRC is presented in Fig. 13. According to this figure, soil layers in borehole no. 1 (BH1) mostly consist of stiff sand and sandy silts, while BH2 comprises of stiff layers of sand at upper elevations underlain by very stiff gravel down to a depth of 30 m. BH3 which is 17 m deep also includes sandy and gravelly soils, while BH4 mostly contains sandy soil with fine particles ultimately reaching to the bedrock at a depth of 12.0 m. In BH5, a clayey layer is detected at upper depths that is underlain by clayey and silty sands.

Figure 14 compares the inverted V_s profiles obtained by conventional and GA-based methods with the results of geophysical seismic refraction and downhole surveys. Among all these methods, downhole survey can be mentioned as the most promising method. Nevertheless, the reliability of this method can even be questionable at larger depths, because of the practical limitations (Apostolidis et al. 2004) and also at very shallow depths due to the complicated wave propagation patterns. As shown in Fig. 14, inverted profiles calculated by both conventional and GA-based methods are generally in agreement with the results of geophysical techniques; however, in some cases, the results are more scattered. At site AR-B1, V_s values obtained by both seismic downhole and refraction tests are in good agreement whereas V_s values predicted by both
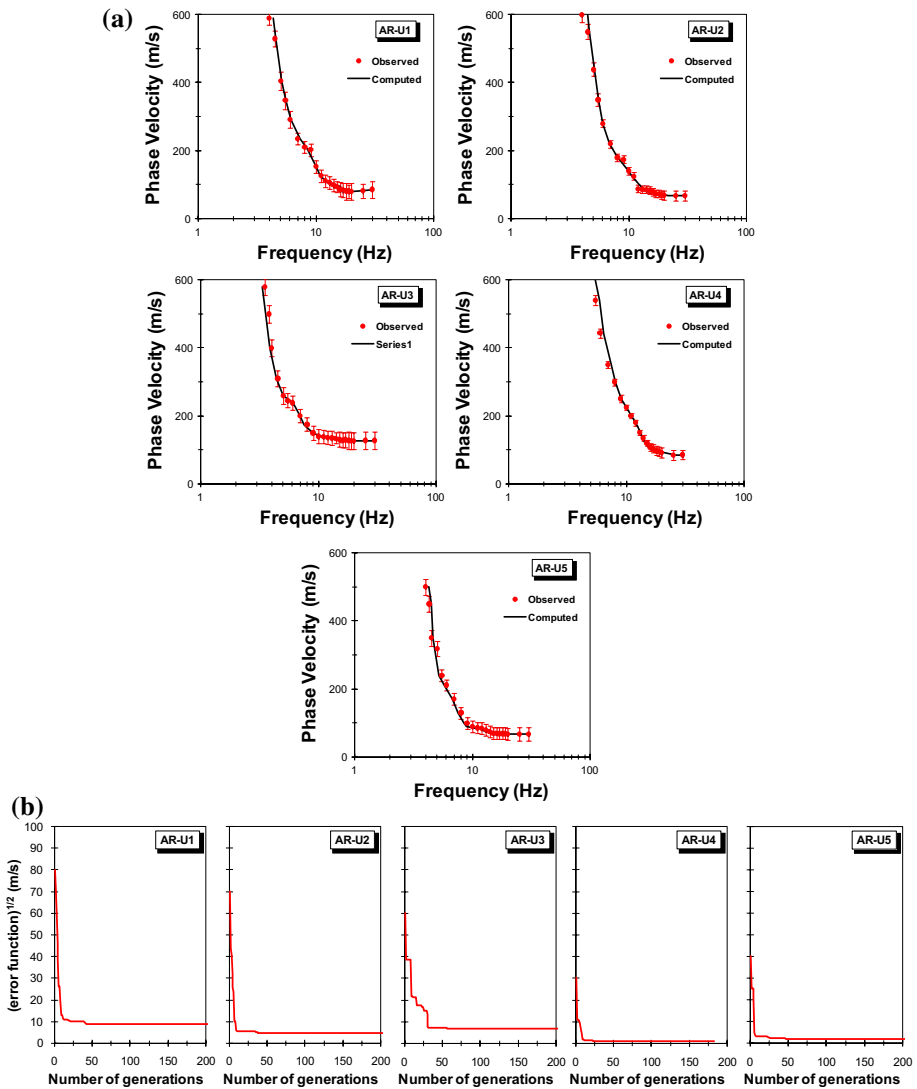
Fig. 11 **a** Experimental and the best-match theoretical dispersion curves for Urmia city (error bars show mean values ± one standard deviation), **b** the corresponding convergence histories

conventional and GA-based methods are generally smaller than those of other methods at top 6–7 m. However, below this shallow depth, the results seem to be more consistent. At site AR-B2, both conventional and GA-based predictions are close to downhole test results at top 5.0 m depths; however, at depths between 5 and 25 m, this agreement is violated. At this depth range, the seismic refraction results appear to be more consistent with the downhole data. At site AR-B3, the results obtained by microtremor and refraction methods are relatively comparable neglecting the top 7~8 m. At site AR-B4, an acceptable agreement can be found between the results of different
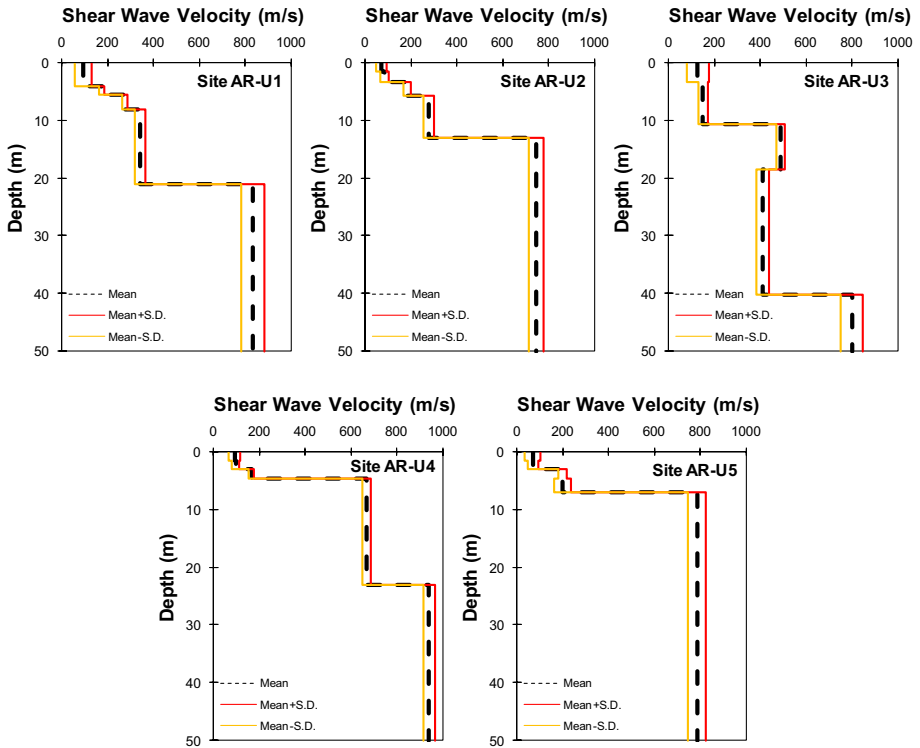
Fig. 12 Inverted V_s profiles in Urmia city obtained by GA-based inversion

methods. In addition, at this site, all methods almost successfully predicted the higher velocity layer at depths deeper than about 10 m previously shown in BH4 log as a bedrock (Fig. 13). At site AR-B5, two V_s profiles provided by the refraction methods are close to each other both showing V_s values greater than those predicted by microtremor methods. However, at depths greater than about 10 m, the GA-based method appears to provide closer results to refraction methods comparing to the conventional method.

Generally speaking, the differences between V_s profiles obtained by different methods are mainly due to the fact that both microtremor and seismic refraction methods estimate the average values of V_s in a limited number of soil layers, while downhole method yields V_s values in shorter sequences providing more continuous variation of V_s versus depth. In order to compare the variability of the results, coefficient of variation of the V_s data provided by different methods was computed as shown in Fig. 15. Note that the coefficient of variation (C.O.V) is defined as the ratio of the standard deviation of a group of V_s data divided by their mean. Referring to Fig. 15, it is revealed that at all sites, the C.O.V values are high at near-surface depths (i.e., less than about 10.0 m) indicating that the results are more scattered. However, at depths deeper than about 10 m, the C.O.V values are smaller than 0.2 indicating that the data provided by different methods are more compatible.
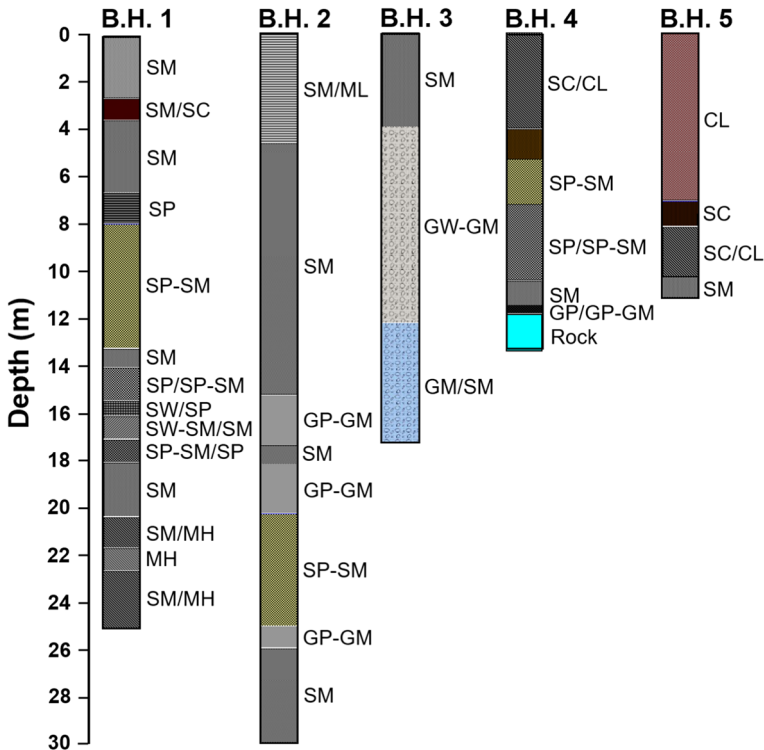
Fig. 13 Geotechnical borehole logs at microtremor array stations in Bam city

3.3.2 Urmia city

Simplified geotechnical logs of five boreholes drilled nearby the microtremor array stations in Urmia city are presented in Fig. 16. As can be seen, at BH1, the 50 m deep ground profile is mainly characterized by fine-grained soil of low plasticity (CL and ML) with a few layers of sand and gravel. BH2 is 40 m deep and mostly consists of clay and silt with low plasticity. In some depths of this borehole, stiff layers of sand and gravel were also encountered. BH3 with 40 m depth mainly includes sandy and gravely layers with a few loose interlayers of clay and silt, while at depths deeper than 35 m, a very stiff gravelly layer is detected. BH4 is drilled to a depth of 40 m and mostly consists of gravel and silty sand, while clayey and silty layers were also found at depths between 19 m and 27 m. BH5 is drilled to a depth of 33 m where a very stiff sandy layer is detected. This location mostly consists of stiff gravel and silty sand where at depths deeper than 25 m, very stiff layers of sand and gravel are observed.

In Fig. 17, the inverted V_s profiles in Urmia city are compared with the results of geotechnical and geophysical seismic refraction methods. The geotechnical method in this figure corresponds to V_s values estimated by an empirical correlation between V_s and N_{SPT} (Baziar et al. 1998) whose general form is presented in Eq. 11. In this equation, N_{SPT} is the SPT blow count and D denotes the depth of the layer in m. The reason for selecting this correlation is its applicability to Iranian in situ SPT data.
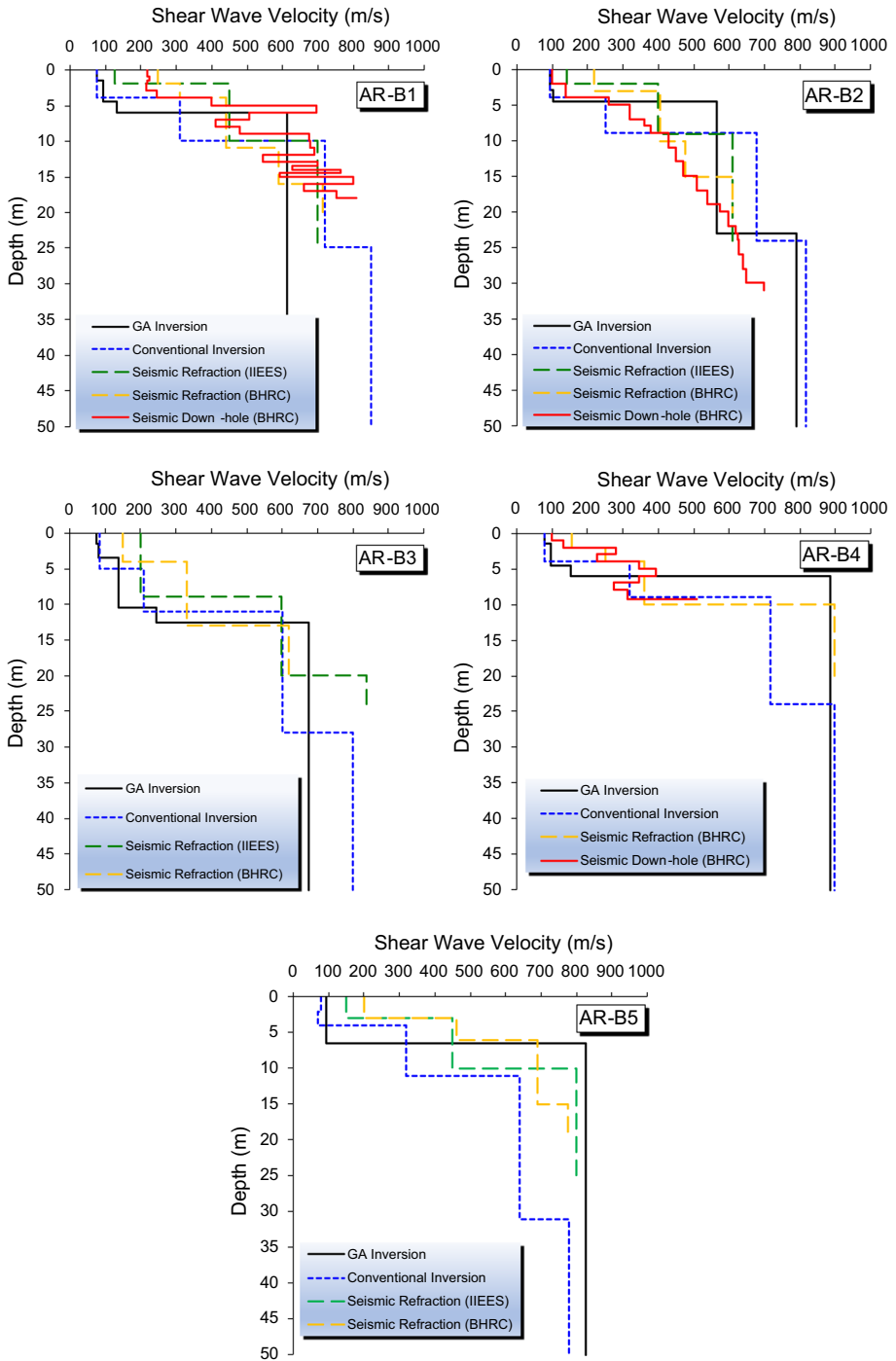
Fig. 14 Comparison between inverted V_s profiles and results of other V_s profiling methods in Bam city
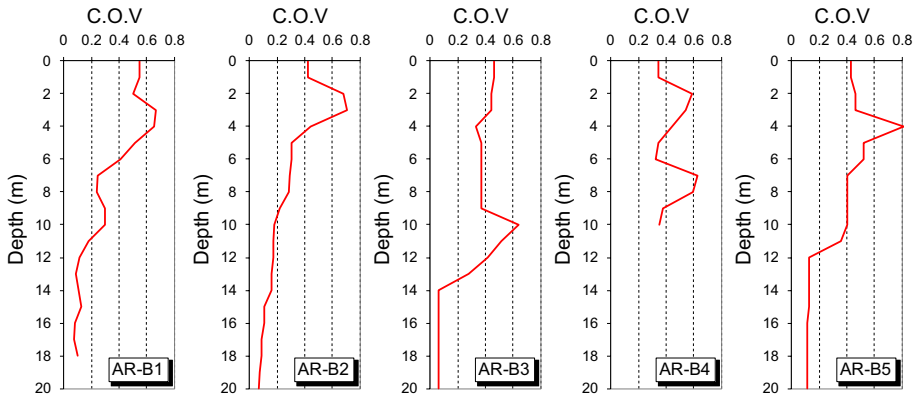
Fig. 15 C.O.V of obtained V_s values versus depth at different locations in Bam city
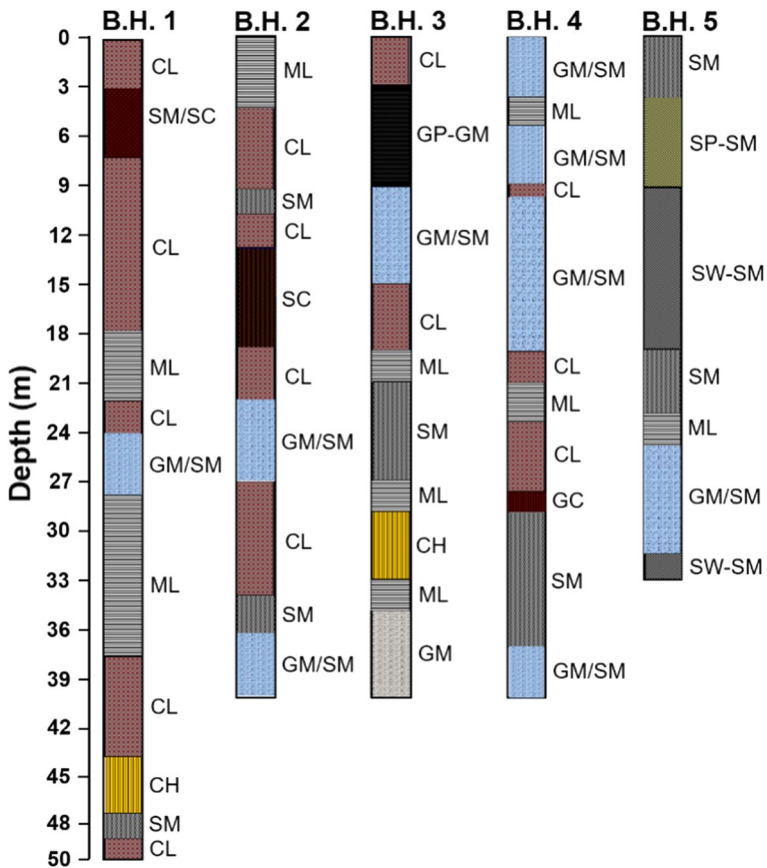

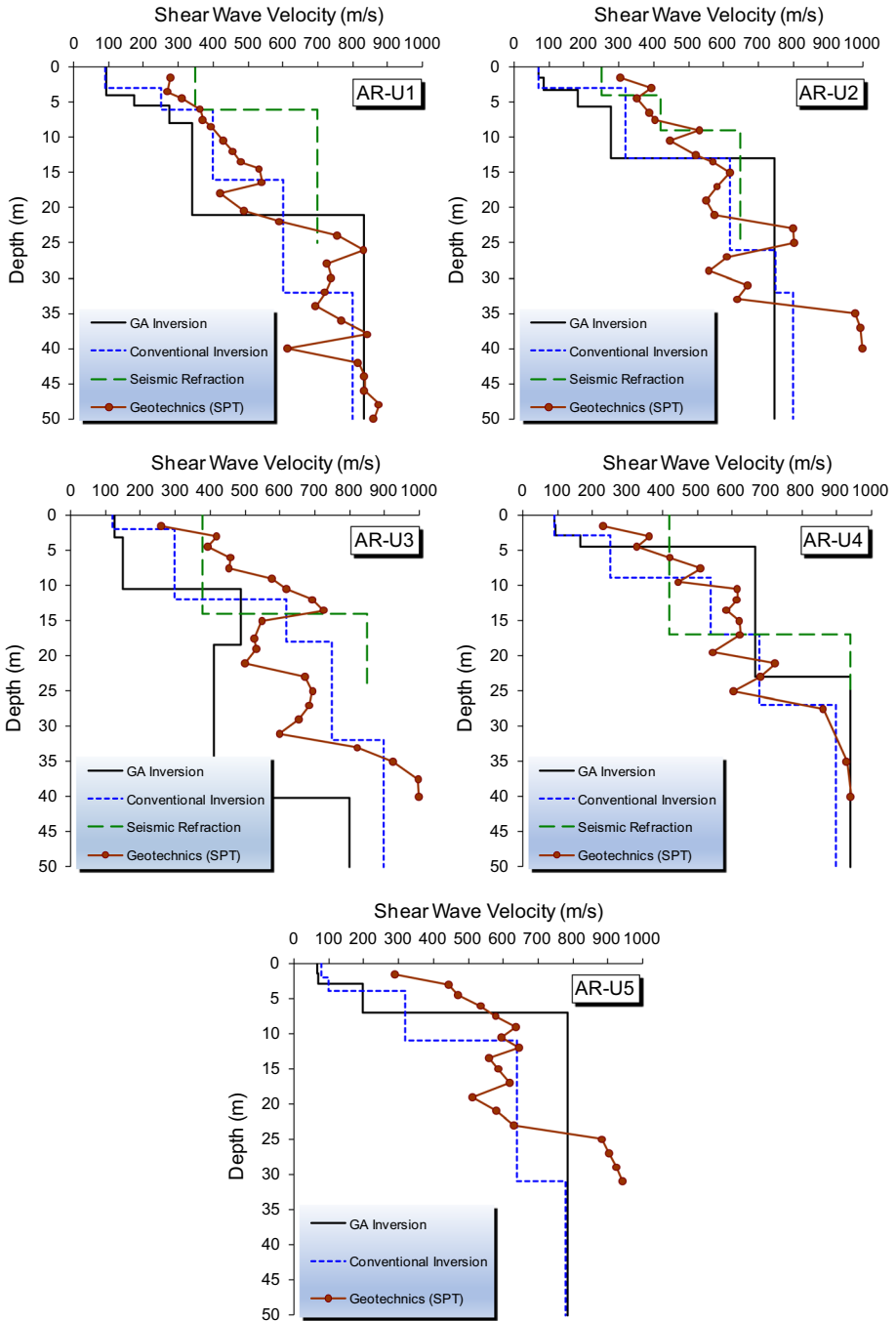**Fig. 16** Geotechnical borehole logs at microtremor array stations in Urmia city

Fig. 17 Comparison between inverted V_s profiles and results of other V_s profiling methods in Urmia city

$$V_s = 134(N_{SPT})^{0.2}(D)^{0.3} \qquad (11)$$

The results presented in Fig. 17 indicate that in most cases, the inverted V_s profiles are relatively in agreement with those determined by other methods. For example, at site AR-U1, the results of both conventional and GA-based methods are in agreement with the values estimated by V_s–N_{SPT} correlation, whereas seismic refraction method yields V_s values far from the other methods at depths smaller than 25 m. At site AR-U2, a good agreement is found between different methods at depths greater than 15 m; however, at the upper 15 m, V_s values read from microtremor methods are smaller than those obtained by seismic refraction and SPT correlation. At site AR-U3, V_s values predicted by conventional inversion, V_s–N_{SPT} correlation and seismic refraction are in general agreement, whereas V_s values obtained by GA-based approach in this site are smaller than those predicted by other methods. This might be due to the fact that although the theoretical and experimental dispersion curves were well matched during the GA-based inversion, the inverted V_s profile in this case was not probably the unique optimum solution to the inverse problem. Nevertheless, GA-based method detected a soft layer under the shallow stiff layer at site AR-U3 which was not identified neither by the conventional inversion method nor by the seismic refraction survey. It is worth noting that the presence of such a soft layer is confirmed by result of the geotechnical investigations at this site (depth 15–30 m). The results of different methods at site AR-U4 are quite consistent, and the agreement is even greater at deeper depths.

A worth noting observation is that at shallow depths, the results of seismic refraction method are generally greater than those predicted by other methods, especially at sites AR-U1, AR-U3 and AR-U4. This is because the thickness of first shallow layer considered in the theoretical model for seismic refraction calculations was not small enough to capture the shallow minor variation of V_s values with depth therefore yielding somewhat an average V_s value for this layer. For site AR-U5, there is no seismic refraction data available; therefore, there may not be a possibility of a robust comparison. Nonetheless, the results of both conventional and GA-based approaches at this site deviate from the N_{SPT}-based predictions particularly within shallow layers of less than 7 m deep.

Figure 18 shows the C.O.V values of V_s data of different methods versus depth. In this figure, the C.O.V values at most sites decrease to values less than about 0.2 at a depth around 10–12 m, while at shallower depths, the C.O.V values are quite large indicating
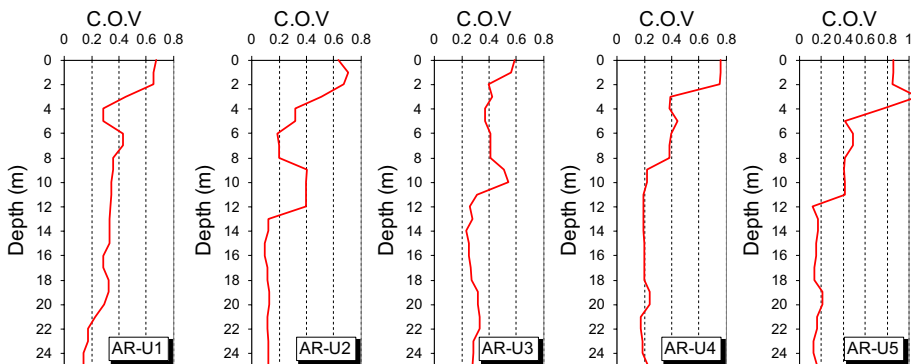

Fig. 18 C.O.V of obtained V_s values versus depth at different locations in Urmia city

that the obtained V_s values are more scattered. These observations confirm that V_s data provided by different methods are more compatible at depths deeper than about 10–12 m.

3.3.3 Further investigations

V_s values of soil layers and their variation with depth are an essential parameter for seismic ground response analysis which in turn significantly affect the predicted ground response (e.g., peak ground acceleration or design response spectrum). On this basis, comparison between seismic ground responses calculated based on each inverted V_s profile can be used to compare the reliability of the employed inversion methods.

Site AR-B2 in Bam city was located at the governor's office of the city where the mainshock acceleration time history of 2003 Bam earthquake was recorded. The geotechnical borehole drilled at this location along with the results of seismic downhole test provides a reliable basis to calculate the ground response. To this end, the acceleration time history recorded at the ground surface was converted to the motion at the engineering seismic bedrock via a deconvolution procedure implementing 1D equivalent-linear ground response analyses using SHAKE software. The back-calculated ground motion at the engineering seismic bedrock was then utilized to determine the response at the ground surface using the inverted V_s data by both conventional and GA-based methods and the seismic refraction techniques. The results of these analyses are provided in Figs. 19 and 20 in terms of the acceleration response spectrum at the ground surface. As one may notice, the results of all methods compare well with each other at period ranges greater than 0.2 s; however, at shorter periods (i.e., smaller than 0.2 s), the results of both GA-based and conventional inversion methods agree well with the results of seismic downhole method, while seismic
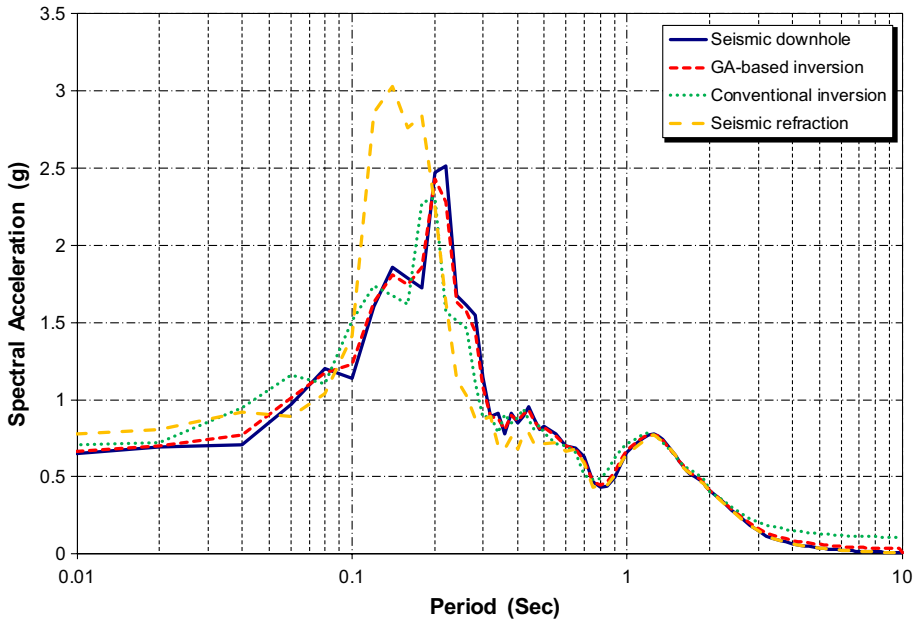

Fig. 19 Response spectrum of N–S component of 2003 Bam earthquake at ground surface
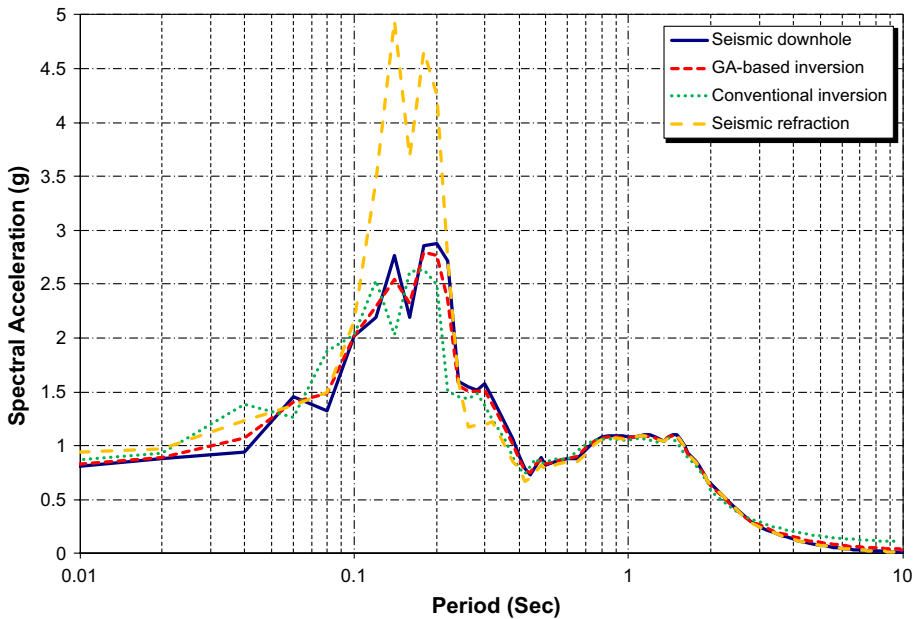
Fig. 20 Response spectrum of E–W component of 2003 Bam earthquake at ground surface

refraction technique shows unrealistic amplifications. This is because the soil layer model in seismic refraction method included only two or three layers with different V_s values which leads to a sharp V_s contrast at the boundary between two successive layers ultimately resulting in more amplification of ground response. On the other hand, seismic downhole or microtremor methods provide more continuous variations of V_s with depth which leads to more realistic estimation of ground response.

An interesting observation in Figs. 19 and 20 is that the peak spectral acceleration occurs in the period range of about 0.15–0.20 s. This period range coincides with the natural vibration period of single story and two-story adobe buildings in central part of Bam city which most of them collapsed or experienced severe damages during the destructive earthquake of December 2003 (Fig. 21).

4 Summary and conclusion

GA-based and conventional derivative-based inversion methods were adopted to obtain V_s profiles of sedimentary deposits by array microtremor measurements in two cities of Iran. For this purpose, inverse analyses of experimental dispersion curves of microtremors were implemented. The reliability of the two inversion procedures is examined, comparing inverted V_s profiles with other available geotechnical and geophysical data in the area. The main findings of the current study can be summarized as follows:

Fig. 21 Severe damages in single story and two-story adobe buildings in central part of Bam city during the destructive earthquake of 2003

1. The results show that V_s profiles obtained by both conventional and GA-based methods are generally in agreement with the results of other V_s profiling techniques. However, this agreement was found to be more at deeper depths.
2. Both conventional and GA-based methods showed lower V_s values at shallower depths comparing to geophysical methods.
3. In both conventional and GA-based inversion methods, the resolution of V_s measurements can be increased by increasing the number of layers for which the V_s values are sought to the extent that extra computational efforts are acceptable. By this consideration, small changes in V_s values can be captured where common geophysical methods such as seismic refraction are not usually capable to detect.
4. The variability of V_s data obtained by different methods was smaller (C.O.V values less than about 0.2) at depths deeper than about 10–12 m, while at shallower depths, the variability was quite large. This indicates that the obtained V_s data were more reliable at greater depths.
5. Comparison between seismic ground responses corresponding to V_s profile obtained by different methods shows that all methods compare well with each other at period ranges larger than 0.2 s in terms of spectral acceleration values; however, at periods smaller than about 0.2 s, the results of both GA-based and conventional inversion and seismic downhole methods agree well with each other, whereas seismic refraction technique shows unrealistic spectral acceleration amplifications.
6. GA-based inversion was relatively slower than the conventional inversion. However, it does not require any initial estimation of unknown parameters as inputs to the search

algorithm. This is an advantage of GA-based methods since conventional inversion algorithms are sensitive to initial estimations where inappropriate initial values can lead to their divergence especially when complicated variation of V_s with depth is encountered.

7. V_s profiling methods utilized in the current study can be used for determination of natural period and amplification ratio of the sediments. This economizes seismic microzonation projects where one series of measurements in each array can simultaneously yield V_s profile, natural period and amplification ratio of the ground.

References

Apostolidis P, Raptakis D, Roumelioti Z, Pitilakis K (2004) Determination of S-wave velocity structure using microtremors and SPAC method applied in Thessaloniki (Greece). Soil Dyn Earthq Eng 24:49–67

Arai H, Tokimatsu K (2004) S-wave velocity profiling by inversion of microtremor H/V spectrum. Bull Seismol Soc Am 94:53–63

Bard P-Y (1999) Microtremor measurements: a tool for site effect estimation? In: Proceedings of the second international symposium on the effects of surface geology on seismic motion, Balkema, Japan, pp 1251–1279

Baziar MH, Fallah H, Razeghi HR, Khorasani MM (1998) The relation of shear wave velocity and SPT for soils in Iran. Paris, France

Capon J (1969) High-resolution frequency-wavenumber spectrum analysis. Proc IEEE 57:1408–1418

Dal Moro G, Pipan M, Gabrielli P (2007) Rayleigh wave dispersion curve inversion via genetic algorithms and Marginal Posterior Probability Density estimation. J Appl Geophys 61:39–55

Dorman J, Ewing M (1962) Numerical inversion of seismic surface wave dispersion data and crust-mantle structure in the New York-Pennsylvania area. J Geophys Res 67:5227–5241

Fernández J, Hermanns L, Fraile A, Alarcón E, del Rey I (2011) Spectral-analysis-surface-waves-method in ground characterization. Procedia Eng 10:3202–3207

Ghalandarzadeh A (2002) Seismic microzonation of Urmia city-phase 1 and 2. Report, Housing and Urban Development Department of West Azarbaijan Province, Iran

Ghalandarzadeh A, Tabatabaii S, Salamat A (2004) Design response spectrum of Bam city. Building and Housing Research Center, Tehran, Iran

Goh TL, Samsudin AR, Rafek AG (2011) Application of spectral analysis of surface waves (SASW) method: rock mass characterization. Sains Malays 40:425–430

Goldberg DE (1989) Genetic algorithms in search, optimization and machine learning. Addison-Wesley Longman Publishing Co., Inc., Boston

Haskell NA (1953) The dispersion of surface waves on multilayered media. Bull Seismol Soc Am 43:17–34

Heisey JS, Stokoe KH II, Hudson WR, Meyer AH (1982) Determination of in situ shear wave velocities from spectral analysis of surface waves. Center for Transportation Research, The University of Texas at Austin, Austin

Holland JH (1975) Adaptation in natural and artificial systems: an introductory analysis with applications to biology, control, and artificial intelligence. University of Michigan Press, Oxford

Horike M (1985) Inversion of phase velocity of long-period microtremors to the S-wave velocity structure down to the basement in urbanized areas. J Phys Earth 33:59–96

Hunaidi O (1998) Evolution-based genetic algorithms for analysis of non-destructive surface wave tests on pavements. NDT and E Int 31:273–280

Kavand A, Ghalandarzadeh A, Tabatabaii S (2006) Determination of shear wave velocity profile of sedimentary deposits in Bam city (southeast of Iran) using microtremor measurements. ASCE Geotech Spec Publ GSP Site Geomater Charact 149:196–203

Kocaoglu AH, Firtana K (2011) Estimation of shear wave velocity profiles by the inversion of spatial autocorrelation coefficients. J Seismol 15:613–624

Kolar P (2000) Two attempts of study of seismic source from teleseismic data by simulated annealing nonlinear inversion. J Seismol 4:197–213

Kuo C-H, Chen C-T, Lin C-M, Wen K-L, Huang J-Y, Chang S-C (2016) S-wave velocity structure and site effect parameters derived from microtremor arrays in the Western Plain of Taiwan. J Asian Earth Sci 128:27–41

Lai CG, Rix GJ (1998) Simultaneous inversion of Rayleigh phase velocity and attenuation for near-surface site characterization. National Science Foundation and U.S. Geological Survey, Georgia Institute of Technology, Atlanta

Liu H, Boore D, Joyner W, Oppenheimer D, Warrick R, Zhang W, Hamilton J, Brown L (2000) Comparison of phase velocities from array measurements of Rayleigh waves associated with microtremor and results calculated from borehole shear-wave velocity profiles. U.S. Department of the Interior, U.S. Geological Surway, USA

Lontsi AM, Ohrnberger M, Krüger F, Sánchez-Sesma FJ (2016) Combining surface-wave phase-velocity dispersion curves and full microtremor horizontal-to-vertical spectral ratio for subsurface sedimentary site characterization. Interpretation 4:41–49

Man KF, Tang KS, Kwong S (2012) Genetic algorithms for control and signal processing. Springer, Berlin

Marano S, Fah D, Lu YM (2014) Sensor placement for the analysis of seismic surface waves: sources of error, design criterion and array design algorithms. Geophys J Int 197:1481–1566

Nakamura Y (1989) A method for dynamic characteristics estimation of subsurface using microtremor on the ground surface. Q Rep RTRI 30:25–33

Pamuk E, Ozdag OC, Tuncel A, Ozyalin S, Akgun M (2018) Local site effects evaluation for Aliaga/Izmir using HVSR (Nakamura technique) and MASW methods. Nat Hazards 90:887–899. https://doi.org/10.1007/s11069-017-3077-y

Pezeshk S, Zarrabi M (2005) A new inversion procedure for spectral analysis of surface waves using a genetic algorithm. Bull Seismol Soc Am 95:1801–1808

Picozzi M, Albarello D (2007) Combining genetic and linearized algorithms for a two-step joint inversion of Rayleigh wave dispersion and H/V spectral ratio curves. Geophys J Int 169:189–200

Rahman MZ, Kamal ASMM, Siddiqua S (2018) Near-surface shear wave velocity estimation and V_s^{30} mapping for Dhaka City. Nat Hazards, Bangladesh. https://doi.org/10.1007/s11069-018-3266-3

Richart FE, Hall JR, Woods RD (1970) Vibration of soils and foundations. Prentice Hall, Englewood Cliffs, p 401

Rix GJ, Stokoe KH, Roesset JM (1991) Experimental study of factors affecting the spectral-analysis-of-surface-waves method

Sahraeian MS, Kavand A, Ghalandarzadeh A (2008) Estimation of shear wave velocity by means of array measurement of microtremors using genetic algorithm method. In: Proceeding of the 14th world conference on earthquake engineering, Beijing, China

Sahraeian MS, Kavand A, Ghalandarzadeh A (2012) Application of genetic algorithm in inversion of Rayleigh waves dispersion curve of array measurement of microtremors. Civ Eng Infrastruct J 45:827–834

Sambridge M (1999) Geophysical inversion with a neighbourhood algorithm—I. Searching a parameter space. Geophys J Int 138:479–494

Shafiee A, Kamalian M, Jafari MK, Hamzehloo H (2011) Ground motion studies for microzonation in Iran. Nat Hazards 59:481–505. https://doi.org/10.1007/s11069-011-9772-1

Singh AP, Parmar A, Chopra S (2017) Microtremor study for evaluating the site response characteristics in the Surat City of western India. Nat Hazards 89:1145. https://doi.org/10.1007/s11069-017-3012-2

Tabatabaii S, Ghalandarzadeh A, Tofigh M, Salamat A (2003) Geotechnical investigations at Iranian strong motion record stations. Building and Housing Research Center, Tehran

Tokeshi K, Harutoonian P, Leo CJ, Liyanapathirana S (2013) Use of surface waves for geotechnical engineering applications in Western Sydney. Adv Geosci 35:37–44

Tokimatsu K (1995) Geotechnical site characterization using surface waves. In: Proceeding of 1st international conference on earthquake geotechnical engineering, The Japanese Geotechnical Society, Japan, Tokyo, pp 1–35

Tokimatsu K, Shinzawa K, Kuwayama S (1992) Use of short-period microtremors for V_s profiling. J Geotech Eng 118:1544–1588

Wu CF, Huang HC (2012) Estimation of shallow S-wave velocity structure in the Puli basin, Taiwan, using array measurements of microtremors. Earth Planets Space 64:389–403

Yamanaka H, Ishida H (1996) Application of Genetic algorithms to an inversion of surface-wave dispersion data. Bull Seismol Soc Am 86:436–444